



CrossMark
click for updates

Cite this: *RSC Adv.*, 2015, 5, 97143

Exploration of using thermally responsive polyionic liquid hydrogels as draw agents in forward osmosis†

Yufeng Cai,^{ab} Rong Wang,^{bc} William B. Krantz,^{bd} Anthony G. Fane^{bc}
and Xiao 'Matthew' Hu^{*ab}

Thermally responsive hydrogels based on ionic liquid monomers of tetrabutylphosphonium *p*-styrenesulfonate (P4444 SS) and tributylhexylphosphonium *p*-styrenesulfonate (P4446 SS) were prepared by bulk polymerization in the presence of a crosslinker, and explored as draw agents in forward osmosis for the first time. Unlike traditional copolymer hydrogels from *N*-isopropylacrylamide (NIPAm) and sodium acrylate (SA) or sodium 2-acrylamido-2-methylpropane sulfonate (AMPS), the combination of thermo-sensitivity and the ionic nature in the hydrogel was achieved by subtle structure design of the ionic liquid monomers. These polyionic liquid hydrogels were proved to be able to generate a reasonable water flux from brackish water, and effectively release the desalinated water at temperatures above their Lower Critical Solution Temperature (LCST). In addition, a set of rational criteria for assessing responsive hydrogel draw agents was proposed, for the first time, to improve the hydrogels' comprehensive performance. Our studies revealed that, both intrinsic factors including hydrogel structure, membrane structure and hydrogel particle–particle contact conditions as well as extrinsic parameters such as the hydrogel's area density on the membrane and FO–regeneration cycle duration, would have a profound impact on the desalination efficacy using hydrogels.

Received 15th September 2015
Accepted 3rd November 2015

DOI: 10.1039/c5ra19018e

www.rsc.org/advances

Introduction

Desalination by forward osmosis (FO) has recently attracted much attention owing to its advantages such as operating at low hydraulic pressure and low membrane fouling propensity.^{1,2} In the FO process, water permeates automatically through a membrane driven by a chemical potential gradient to dilute the draw agent, and fresh water is then separated from the draw agent in the regeneration process. Among all the draw agents developed to date,^{1,3,4} the majority of them are dissolved^{5–10} or dispersed^{11–13} in water to make an aqueous draw solution. Therefore, in order to obtain high quality water and minimize draw agent loss, additional processes including nanofiltration (NF), reverse osmosis (RO) or (membrane) distillation are indispensable as the final step regardless of any possible previous separation by external stimuli in the draw agent

regeneration process.^{5,10,12} Undoubtedly, these would bring in additional equipment and energy costs for FO desalination.

Hydrogels are crosslinked polymers with water entrapped within the network. Directly immersing hydrogel in brackish water has been proved to only achieve a low desalination efficiency.^{14,15} However in FO, a membrane separates hydrogels (the draw agents) from brackish water so that hydrogels were swollen by desalinated water due to water chemical potential gradient across the membrane.^{16,17} The advantages of hydrogels as draw agents include no draw agent loss or back diffusion, and most importantly, hydrogels can easily release desalinated water by shrinking network under external stimulus like temperature change, therefore exempting any further tedious membrane-based water polishing processes. Poly-*N*-isopropylacrylamide (PNIPAm) based hydrogels have been intensively studied as draw agents.¹⁸ Neat PNIPAm hydrogel can swiftly release entrapped water at temperatures above LCST in regeneration process due to its thermo-sensitivity. However, its performance in FO process at temperatures below LCST is quite poor owing to its non-electrolyte nature. Randomly copolymerizing NIPAm with electrolyte, *i.e.*, sodium acrylate, would annihilate thermo-sensitivity of the copolymer hydrogel¹⁹ albeit the water flux generated in FO process increases.¹⁸

Organic and inorganic fillers including black carbon particles,²⁰ graphene²¹ and Fe₃O₄ (ref. 22) have been incorporated into the NIPAm–SA copolymer hydrogels to enhance deswelling

^aSchool of Materials Science and Engineering, Nanyang Technological University, 50 Nanyang Avenue, Singapore 639798. E-mail: asxhu@ntu.edu.sg

^bNanyang Environmental & Water Research Institute, 1 Cleantech Loop, Singapore

^cSchool of Civil & Environmental Engineering, Nanyang Technological University, 50 Nanyang Avenue, Singapore 639798

^dDepartment of Chemical and Biological Engineering, University of Colorado, USA

† Electronic supplementary information (ESI) available. See DOI: 10.1039/c5ra19018e

performance. However, since the NIPAm-SA copolymer hydrogel matrix is still not thermally responsive, majority of the water released was in vapor state due to evaporation under heat, albeit the heat was smartly indirectly generated from solar energy or magnetic induction. Recently, electro- and magnetic responsive hydrogels were also tested as draw agents.^{23,24} All of the hydrogels serving as draw agents face the compromise between performances in FO process and regeneration process. However, in almost all the papers published on hydrogel draw agents, the FO process and regeneration process were studied separately and never evaluated in a comprehensive FO-regeneration cyclic continuous process perspective with few exceptions.^{25,26} For example, FO performance was always evaluated by water flux generated by hydrogels from completely dry state that cannot be recovered after regeneration process. Our group once came up with PNIPAm-based semi-IPN hydrogel to increase the water flux in FO process without jeopardizing thermo-sensitivity, and demonstrated preliminary concept in assessing hydrogel's FO-regeneration comprehensive performance.²⁶ However, the relatively low water flux of ~ 0.2 LMH still left room for further improvement. What's more, the absence of a systematic criterion to judge a hydrogel's comprehensive performance hinders the progress of exploring more competent hydrogels as draw agents.

In this work, we discarded the traditional NIPAm-electrolyte copolymer hydrogel system and managed to blend hydrophilicity and hydrophobicity into sole monomer of a thermally responsive ionic liquid tetrabutylphosphonium *p*-styrenesulfonate (P4444 SS). Thermally responsive polyionic liquid hydrogel can be easily synthesized by polymerizing and crosslinking this novel ionic liquid, and tuned by copolymerizing with other ionic liquids. We scrutinized the influences on the water production rate from both intrinsic factors including hydrogel structure, membrane structure as well as hydrogel particle-particle contact conditions and extrinsic parameters such as hydrogel's area density on membrane and FO-regeneration cycle duration. In addition, a systematic judging criterion was proposed for the first time to help improve hydrogel draw agents' performances.

Experimental

Materials

N-Isopropylacrylamide (NIPAm, $\geq 98\%$) was purchased from Wako Pure Chemical Industrials Ltd. (Japan). *N,N'*-Methylenebis(acrylamide) ($\geq 99\%$), polyvinyl alcohol (PVA, $M_w = 61\,000\text{ g mol}^{-1}$), *N,N,N',N'*-tetramethylethylenediamine (TEMED, 99%), benzophenone ($\geq 99\%$) and dichloromethane ($\geq 99\%$) were purchased from Sigma-Aldrich. Ammonium peroxydisulfate (98%) and polyethylene glycol dimethacrylate ($M_w = 198\text{ g mol}^{-1}$) were purchased from Alfa Aesar. Tetrabutylphosphonium bromide ($>99\%$) and sodium *p*-styrenesulfonate ($>98\%$) were purchased from Tokyo Chemical Industry Ltd. Tributylhexyl phosphonium bromide was purchased from Sino Rarechem Labs. All chemicals were used directly without any purification. Two kinds of FO membranes were received from Hydration Technology Innovations (HTI) and synthesized according to a literature,²⁷ respectively.

Preparation of ionic liquid monomer

Tetrabutylphosphonium *p*-styrenesulfonate (P4444 SS) was synthesized by ion exchange. In a typical synthesis, 20 g of tetrabutylphosphonium bromide and 17.7 g of sodium *p*-styrenesulfonate were dissolved in 30 ml of deionized (DI) water and the homogeneous solution was stirred for 24 hours before 80 ml of dichloromethane was added to extract the ionic liquid. The dichloromethane phase was washed with 20 ml DI water for three times. The dichloromethane was evaporated under high vacuum (<0.1 mbar) at room temperature for 72 hours. The synthesis of tributylhexyl phosphonium *p*-styrenesulfonate (P4446 SS) was conducted in a similar method. 20 g of tributylhexyl phosphonium bromide and 16.3 g of sodium *p*-styrenesulfonate were dissolved into 30 ml water. The solution turned into opaque suspension since the target ionic liquid P4446 SS is hydrophobic. After 24 hours stirring, the ionic liquid was extracted by 80 ml dichloromethane and washed with 20 ml DI water for three times. The ionic liquid was purified at high vacuum for 72 hours. Both P4444 SS and P4446 SS are stored at $-22\text{ }^\circ\text{C}$ to avoid polymerization. The structures and NMR spectra of these two ionic liquids were demonstrated in Fig. 1. P4444 SS: ^1H NMR, δ_{H} (400 MHz, CDCl_3): 0.89–0.93 (t, 12H, CH_3), 1.43–1.45 (m, 16H, CH_2), 2.23–2.25 (m, 8H, CH_2), 5.19–

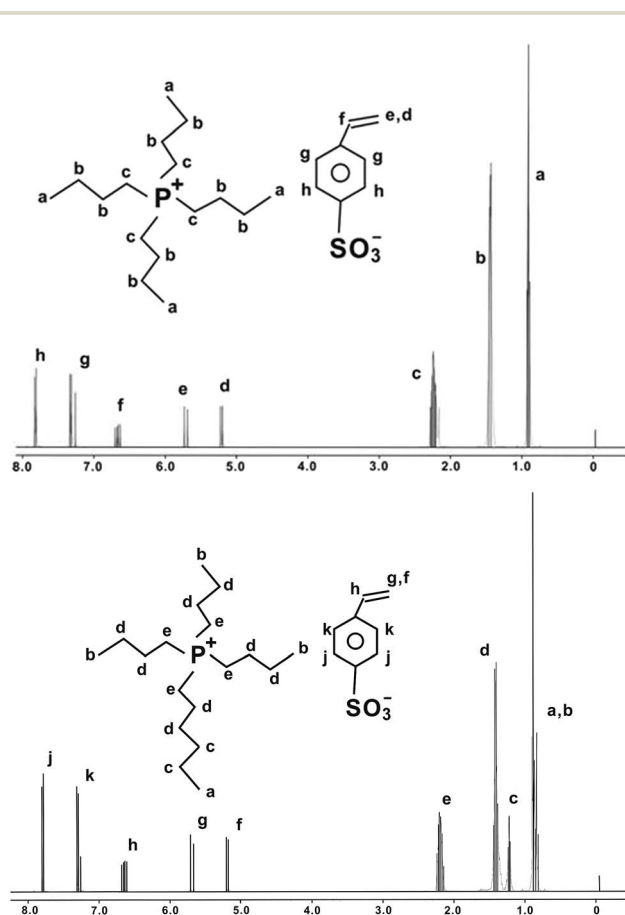


Fig. 1 Molecular structures and NMR spectra of (upper) tetrabutylphosphonium *p*-styrenesulfonate (P4444 SS) and (lower) tributylhexylphosphonium *p*-styrenesulfonate (P4446 SS).

5.22 (d, 1H, CH), 5.69–5.73 (d, 1H, CH), 6.63–6.68 (q, 1H, CH), 7.26–7.34 (d, 2H, CH), 7.81–7.83 (d, 2H, CH) ppm. P4446 SS: ^1H NMR, δ_{H} (400 MHz, CDCl_3): 0.83–0.85 (t, 3H, CH_3), 0.88–0.90 (t, 9H, CH_3), 1.19–1.22 (m, 4H, CH_2), 1.39–1.43 (m, 16H, CH_2), 2.18–2.21 (m, 8H, CH_2), 5.18–5.20 (d, 1H, CH), 5.67–5.71 (d, 1H, CH), 6.63–6.68 (q, 1H, CH), 7.26–7.34 (d, 2H, CH), 7.81–7.83 (d, 2H, CH) ppm.

Synthesis of poly ionic liquid hydrogels

The PNIPAm and PNIPAm–PVA semi-IPN hydrogels were synthesized according to our previous publication.²⁶ For the synthesis of poly ionic liquid hydrogel poly(tetrabutylphosphonium *p*-styrenesulfonate) (PP4444 SS), 44.8 mg (0.226 mmol) of crosslinker polyethylene glycol dimethacrylate ($M_n = 198 \text{ g mol}^{-1}$) and 20.6 mg (0.113 mmol) of photo-initiator benzophenone were dissolved in 5 g (11.3 mmol) P4444 SS. The homogenous solution was purged with N_2 for 15 minutes and the polymerization was conducted under UV (365 nm, 54 mW cm^{-2}) for 2 hours. The copolymer hydrogel of P4444 SS with 20 mol% of P4446 SS (PP444-6 SS) were synthesized in a similar method. The crosslinker and photo-initiator used were still 2 mol% and 1 mol%, respectively with respect to monomers. The poly-ionic liquid hydrogel syntheses were shown in Fig. 2. All the hydrogels were allowed to swell to equilibrium to leach unreacted molecules and then dried until constant weight before ball milled into powders ready for use. The dimension of the dried hydrogel particle is less than $30 \mu\text{m}$.

Characterizations

The morphology of FO membranes was characterized by FESEM (JEOL, 6340F). The LCST of each hydrogel was determined by a differential scanning calorimeter (TA Q10 Modulated DSC, TA Instruments). The hydrogels were swollen to a swelling ratio of about 3 g g^{-1} before the DSC measurement. For each DSC measurement, approximately 20 mg of swollen hydrogel was placed into a hermetically sealed aluminum pan. The

temperature range was from 10 to $75 \text{ }^\circ\text{C}$ at a heating rate of $3 \text{ }^\circ\text{C min}^{-1}$. Dry nitrogen was used for purging at a flow rate of 50 ml min^{-1} . The swelling ratio, water flux and deswelling performance of hydrogel were studied by utilizing gravimetric method. In FO process, dry hydrogel powders or discs (formed by particles under pressure of 200 MPa) were put onto FO membrane with selective layer facing the hydrogel. The FO process was conducted at $23 \pm 1 \text{ }^\circ\text{C}$. The water flux J_v (litre per square meter per hour, LMH) was determined by the hydrogel weight increment given time and FO membrane area.

$$J_v = \Delta W / (A \Delta t \rho)$$

where ΔW (g) is the weight increase of the hydrogel, A is the membrane area (m^2), Δt (h) is the FO duration and ρ (g L^{-1}) is the water density. 2000 ppm NaCl solution was used feed solution throughout this work.

Hydrogel's swelling ratio was defined as $\text{SR} = m_{\text{water}}/m_{\text{dry}}$, where m_{water} is the weight of absorbed water within hydrogel while m_{dry} is weight of dry hydrogel. Hydrogel's deswelling was conducted by putting 2 g swollen hydrogel ($\text{SR} \sim 3.8 \text{ g g}^{-1}$) on the surface of $60 \text{ }^\circ\text{C}$ hotplate and monitoring hydrogel's weight change with deswelling time. The hydrogel was covered by wiper (kimwipes) to absorb the released liquid water. The wiper was weighed to determine the amount of liquid water released and it was replaced whenever the hydrogel's weight was measured.

Results and discussion

FO performances of the hydrogels

Fig. 3 demonstrated the water flux and swelling ratio profiles as function of FO process duration of each hydrogel in powder form with cellulose triacetate (CTA) membrane. For each hydrogel as draw agent, the water flux decays and swelling ratio ascends as time elapsed in FO process. The PNIPAm hydrogel, doubtlessly, shows the weakest drawing ability that the initial water flux generated from dry state was only below 0.8 LMH

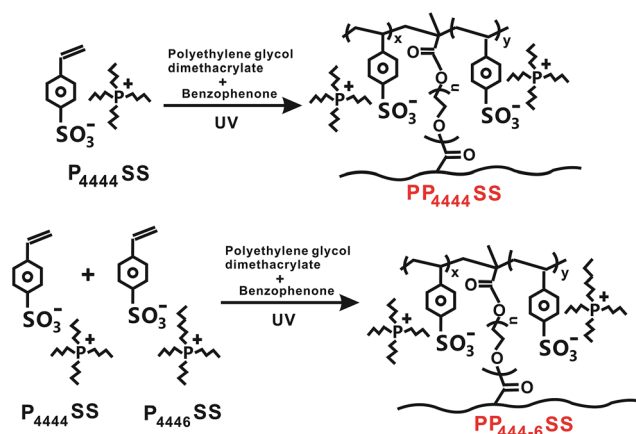


Fig. 2 The synthesis route of polyionic liquid hydrogels. Polyethylene glycol dimethacrylate is crosslinker, and benzophenone is the photo-initiator. The polymerization and crosslinking were conducted in bulk state without solvent.

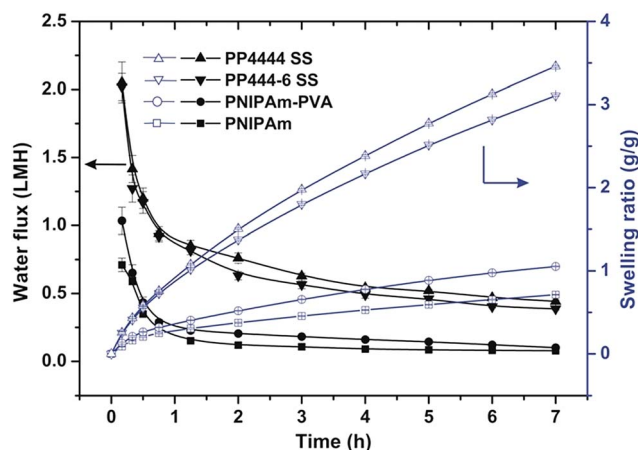


Fig. 3 The water flux and swelling ratio profile of each thermally responsive hydrogel from dry state. The hydrogels were in powder form contacting CTA membrane from HTI with an area density of 0.6 g/4.5 cm^2 .

and the plateau water flux after one hour FO was reduced to below 0.1 LMH. The incorporation of linear hydrophilic PVA into PNIPAm network slightly improved the water flux, albeit the swelling ratio of the semi-IPN hydrogel was still only about one (~ 50 wt% water) after seven hours. This is because any hydrophilic modifications, *e.g.*, incorporating linear polyvinyl alcohol or polysodium acrylate (PSA) into the PNIPAm network, cannot overwhelm the dominance of PNIPAm presence in order to preserve thermo-sensitivity and thus the water flux improvement is limited. In order to further increase thermally responsive hydrogels' performance in FO process, a new route other than copolymerization or semi-IPN to blending hydrophobicity and hydrophilicity in a hydrogel is needed. Replacing the cationic sodium of electrolyte sodium *p*-styrenesulfonate with a more hydrophobic phosphonium cation, the synthesized ionic liquid P4444 SS has achieved hydrophobicity and hydrophilicity coalition in monomer level, and its thermally responsive homopolymer hydrogel demonstrated significantly improved performance in FO process. The initially generated water flux was higher than 2 LMH and after 7 hours the decayed plateau flux could be maintained at about 0.5 LMH. Similar with PNIPAm, this thermally responsive polyionic liquid hydrogel with much better FO performance can also be copolymerized with other species to tune the properties. As can be seen in Fig. 3, after copolymerizing with 20 mol% of hydrophobic P4446 SS, the swelling ratio as well as water flux of PP444-6 SS decreased due to declined hydrophilicity.

A hydrogel's performance in FO process can also be qualitatively characterized by plotting water flux generated at various swelling ratios, as shown in Fig. 4. Obviously, hydrogel with desired FO performance should generate a very high water flux from dry state and the water flux declines insignificantly as swelling ratio increases. The PNIPAm-based hydrogels can only generate initial water flux of ~ 1 LMH, which quickly falls below 0.1 LMH when hydrogel is swollen to swelling ratio of only about 1 g g^{-1} . The PP4444 SS, however, not only generates higher initial water flux of more than 2 LMH, but maintain

a reasonable water flux of ~ 0.5 LMH even at the swelling ratio of 4 g g^{-1} . The improved FO performance of polyionic liquid hydrogels may be accredited to ~ 20 times higher equilibrium swelling ratios than those of PNIPAm-based hydrogels, as shown in Fig. 4 inset. Higher equilibrium swelling ratio indicates more clearance for water chemical potential reduction, therefore, imparts hydrogel the ability to generate higher water flux at the same swelling ratio. In order to fully exert their potential capacity in FO process, other aspects influencing water diffusion such as hydrogel particle-particle contact conditions and FO membrane have also been scrutinized. PP4444 SS and PP444-6 SS demonstrated improved FO performances when the hydrogel powders were compressed into disc form and cellulose triacetate membrane from HTI was replaced with thin film composite (TFC) membrane as shown in Fig. S1, ESI†. This is because that water diffusion from feed solution to hydrogel has been facilitated by using thinner membrane (Fig. S2, ESI†), and the compressed interstitial volume between particles in the disc improves the inter-particle contact condition and water diffusion.²⁸ As shown in Fig. 4, after optimization in water diffusion facilitation, PP4444 SS can generate initial water flux of higher than 4 LMH and maintain it at ~ 2.5 LMH at swelling ratio of 1 g g^{-1} , while PNIPAm-PVA in powder form can only generate ~ 0.1 LMH at the same swelling ratio with CTA membrane.

Regeneration performance of hydrogels

An ideal hydrogel as draw agent in FO not only should generate a high water flux, but can easily and swiftly release the absorbed water to make the desalinated water available. The hydrogel's swelling ratio reduction at 60°C and LCSTs were shown in Fig. 5 and 6. The subtle balance between hydrophilicity and hydrophobicity imparts thermo-sensitivity to the PP4444 SS with a LCST of 58.7°C . Thus, the swelling ratio of PP4444 SS can reduce from 3.8 g g^{-1} to 1.7 g g^{-1} after 15 minutes at 60°C . It is worth noting that the LCST peaks of polyionic liquid hydrogels are quite broad,²⁹ deswelling temperature of 60°C falls into the

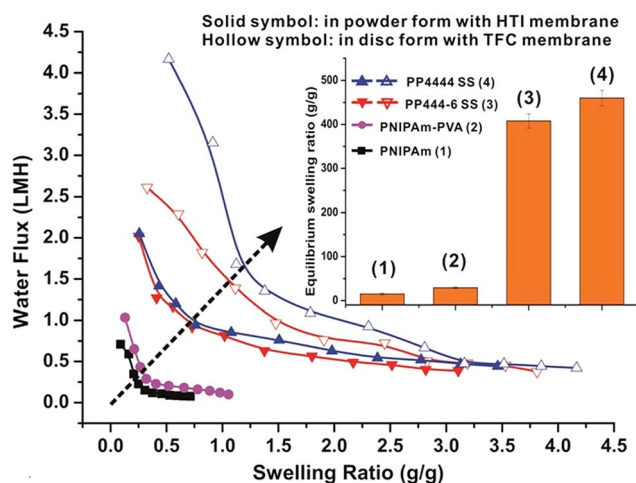


Fig. 4 The swelling ratio and the corresponding generated water flux correlation of each thermally responsive hydrogel. Inlet was the equilibrium swelling ratio of each hydrogel immersing in DI water.

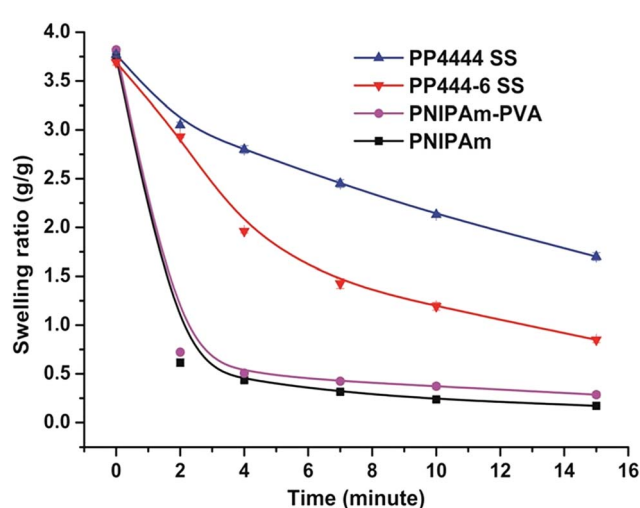


Fig. 5 Swelling ratio profiles of each thermally responsive hydrogel in regeneration process.

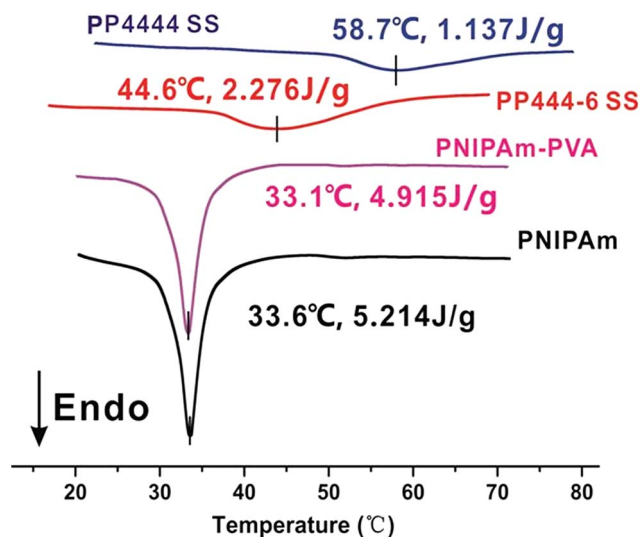


Fig. 6 The LCSTs and latent heat during phase change of each hydrogel.

peak region of PP4444 SS and may not be high enough to guarantee complete phase transition. Instead of increasing deswelling temperature to achieve faster hydrogel regeneration, declining the hydrogels' LCSTs would be a more feasible and attractive method. After copolymerizing with 20 mol% more hydrophobic P4446 SS, the polyionic liquid hydrogel PP444-6 SS has an acceptable LCST of $\sim 44^\circ\text{C}$ and deswelling temperature of 60°C locates above the entire phase separation peak. Therefore, PP444-6 SS has better deswelling performance than PP4444 SS that it can reach a swelling ratio of 0.85 g g^{-1} after 15 minute deswelling. Actually besides the LCST, the deswelling process of hydrogels can also be depicted by the phase transition heat. This energy input is an indication of the extent or severity of the thermally responsive hydrogels' structural change including bound water to free water transition and hydrophobic association, *etc.*³⁰ Therefore, hydrogels like PSA and its copolymer with NIPAm assuming no phase transition would make the majority of water released at high temperature in vapor form, while typical thermally responsive PNIPAm and PNIPAm-PVA have very high transition heat inputs indicating very strong phase transition at LCST, resulting in a quite high liquid water recovery ($>80\%$) since the water was majorly squeezed out (Fig. S3, ESI[†]). Although the polyionic liquid hydrogels may have a unique phase transition mechanism,³¹ the rule that incorporating more hydrophobic segments into polymer backbone reduces LCST also applies. The PP444-6 SS demonstrated not only reduced LCST but increased transition heat compared with pure PP4444 SS hydrogel. Therefore, the recovered liquid water fraction of PP444-6 SS was increased to $\sim 50\%$ albeit still lower than those of PNIPAm-based hydrogels.

Criterion for assessing hydrogel's comprehensive performance

The required abilities of hydrogels as draw agents to generate high water flux in FO process and easily release absorbed water

in regeneration process are always contradictory. Increasing the drawing ability in FO process inevitably jeopardizes the deswelling properties in regeneration process. As can be seen in Fig. 3 that the FO performance ascends in the order of PNIPAm < PNIPAm-PVA < PP444-6 SS < PP4444 SS, while the performance in regeneration process descends in the order of PNIPAm > PNIPAm-PVA > PP444-6 SS > PP4444 SS, as seen in Fig. 5. This compromise also appeared in all the previous published papers about hydrogels as draw agents,^{18,20,22,32} where the FO and dewatering performances were discussed separately and never considered together to evaluate the overall performance in a comprehensive manner. The question of "which hydrogel performs better" was never answered in those papers.

Fig. 7 is the schematic of the universal criterion of hydrogel's comprehensive performance as draw agent in FO desalination. Since all the thermally responsive hydrogels cannot retain their completely dry state after deswelling process, the hydrogel would start the next FO process with a swelling ratio of SR_0 obtained after the deswelling in regeneration process. All the water absorbed in the FO process with hydrogel starting from swollen state (SR_0) could be released in regeneration process to make the FO-regeneration cycle reversible, and the water flux calculated in this criterion depicts the desalinated water production rate rather than the water absorbing rate in sole FO process. For example, after knowing the fitting function of the correlation between swelling ratio and FO time of each hydrogel (Fig. S4, ESI[†]), we can easily calculate the increment of swelling ratio (ΔSR) from SR_0 in FO process whose duration is T_{FO} . The duration of regeneration process ($T_{\text{des.}}$) should be long enough to restore SR_0 . Then the desalinated water production rate can be calculated given the dry hydrogel weight and total duration of one FO-regeneration cycle.

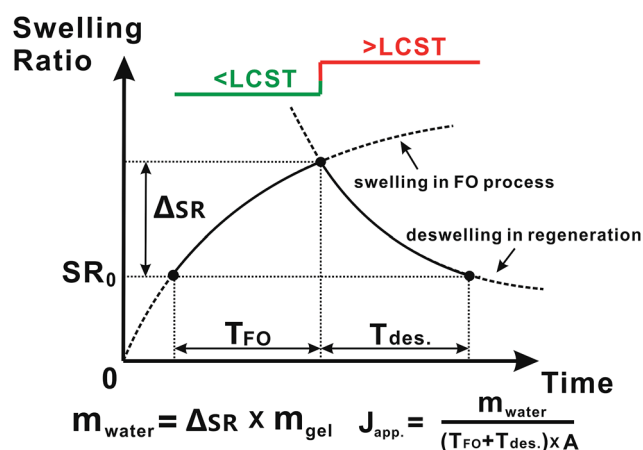


Fig. 7 The schematic illustration of criterion for hydrogel's comprehensive performance in reversible FO-regeneration cycles. T_{FO} and $T_{\text{des.}}$ are the duration of FO process and regeneration process, respectively. SR_0 is swelling ratio obtainable after regeneration, which can be found in Fig. 5 for each hydrogel. A is the active membrane area that is 4.5 cm^2 in this work. ΔSR is the swelling ratio increment during the FO process and m_{gel} is the weight of dry hydrogel. m_{water} is the amount of water absorbed that can also be fully released during regeneration process in one cycle. Therefore, the apparent water flux ($J_{\text{app.}}$) calculated in this criterion is the water production rate.

The influence of hydrogel's composition, membrane structure and hydrogel contact condition

We use the established criterion to assess the comprehensive performance of hydrogels as draw agents for the rest of this paper. If we fix one FO-regeneration cycle within one hour, the swelling ratio profiles of each thermally responsive hydrogel within one FO-regeneration cycle were demonstrated in Fig. 8 and the key parameters of the criterion were summarized in Table 1. The PNIPAm's inherently poor drawing ability makes the lowest desalinated water production rate of 0.18 LMH though the hydrogel's swelling in FO process starts from a almost dry state ($SR_0 = 0.17 \text{ g g}^{-1}$). The incorporation of hydrophilic linear PVA only slightly improves the comprehensive performance with a water production rate of 0.22 LMH. The PP4444 SS can generate the highest water flux from dry state as mentioned above, however, its relatively poor deswelling performance resulted in the highest swelling ratio after deswelling ($SR_0 = 1.70 \text{ g g}^{-1}$), which in turn paralyzed its FO performance in cyclic perspective. More balanced FO and regeneration performances achieved by PP444-6 SS make it the best draw agent for FO desalination that can achieve a desalinated water production rate of 0.61 LMH. In addition, as mentioned, the water diffusion from brackish water into hydrogels also hinges on the barriers from membrane structure and hydrogel particle-particle contact condition. After using a thinner membrane and improving the hydrogel contact condition by compressing it into disc form, the water production rate of PP444-6 SS can be further enhanced to 0.94 LMH.

The influence of hydrogel area density and one FO-regeneration cycle duration

The hydrogel PP444-6 SS with the best comprehensive performance among all the thermally responsive hydrogels was selected to achieve a higher desalinated water production rate by tuning the hydrogel area density (weight of hydrogel/area of membrane). Fig. S5† shows that the swelling ratio of a hydrogel

Table 1 Influence of hydrogel composition, membrane structure and hydrogel particle-particle contact conditions on comprehensive performance as draw agents^a

	PNIPAm	PNIPAm-PVA	PP4444 SS	PP4444 SS*	PP444-6 SS	PP444-6 SS*
T_{FO} (min)	52	51	55	52	53	50
$T_{des.}$ (min)	8	9	5	8	7	10
SR_0 (g g^{-1})	0.17	0.28	1.70	1.70	0.85	0.85
ΔSR (g g^{-1})	0.134	0.161	0.409	0.574	0.459	0.702
m_{water} (mg)	80.4	96.6	245.4	344.4	275.4	421.2
$J_{app.}$ (LMH)	0.18	0.22	0.55	0.77	0.61	0.94

^a The entire one FO-regeneration duration is one hour. Hydrogels without asteroid mark were using CTA membrane in powder form. Hydrogels with asteroid mark were using TFC membrane in disc form.

with a smaller area density would increase faster than that of a hydrogel with a larger one. This has been reported and was probably due to the influence of water diffusion path length through the hydrogel.^{26,28} On a fixed membrane area and within fixed FO time, less amount of hydrogel would lead to larger swelling ratio increment, while the amount of water is calculated by the swelling ratio increment multiplying weight of dry hydrogel. Therefore, there exists a best hydrogel area density that maximizes the amount of water produced. Again, we fitted the correlation between swelling ratio and FO time of PP444-6 SS (in disc form with TFC membrane) with different area densities (Fig. S6, ESI†) and fixed one FO-regeneration cycle in one hour to compare the desalinated water production rate. The swelling ratio profiles within one FO-regeneration cycle was demonstrated in Fig. 9 and the key parameters in the criterion were summarized in Table 2. It can be observed that although the area density of $0.09 \text{ g}/4.5 \text{ cm}^2$ can generate the highest swelling ratio increment, yet the area density of $0.2 \text{ g}/4.5 \text{ cm}^2$ produces the largest amount of water within one FO-regeneration cycle and the highest desalinated water

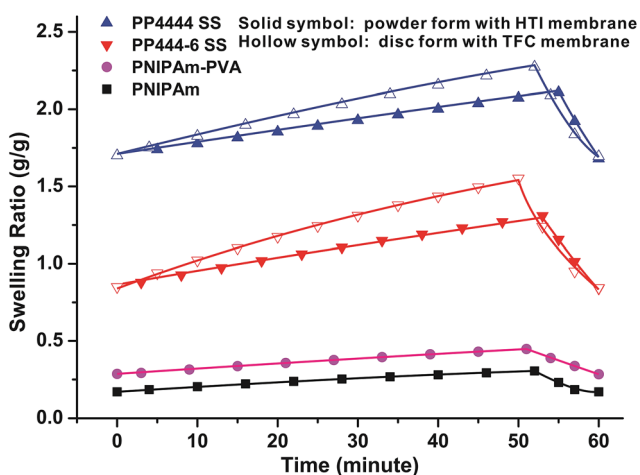


Fig. 8 Comparison of comprehensive performance of each hydrogel in one reversible FO-regeneration cycle within one hour. Area density was $0.6 \text{ g}/4.5 \text{ cm}^2$.

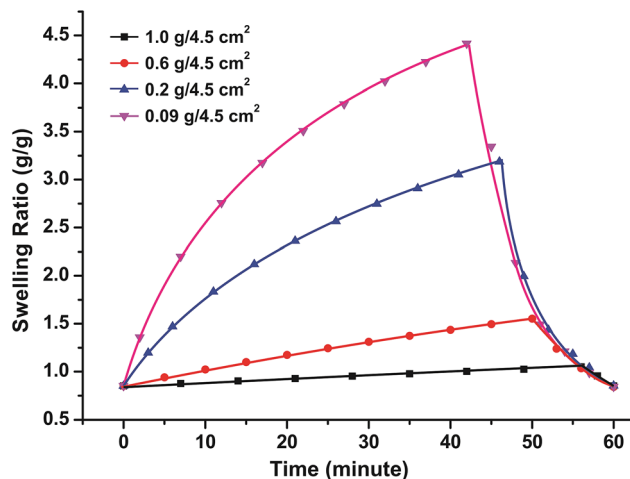


Fig. 9 The influence of hydrogel area density on the comprehensive performance. The hydrogel was PP444-6 SS in disc form contacting TFC membrane.

Table 2 Influence of hydrogel area density on the water production rate of PP444-6 SS^a

	1.0 g/4.5 cm ²	0.6 g/4.5 cm ²	0.2 g/4.5 cm ²	0.09 g/4.5 cm ²
T_{FO} (min)	56	50	46	42
$T_{des.}$ (min)	4	10	14	18
SR_0 (g g ⁻¹)	0.85	0.85	0.85	0.85
ΔSR (g g ⁻¹)	0.199	0.702	2.337	3.568
m_{water} (mg)	199.0	421.2	467.4	321.1
$J_{app.}$ (LMH)	0.44	0.94	1.04	0.71

^a The hydrogel was in disc form contacting TFC membrane.

Table 3 The comprehensive performance of PP444-6 SS with one FO–regeneration cycle fixed within 30 minutes^a

	1.0 g/4.5 cm ²	0.6 g/4.5 cm ²	0.2 g/4.5 cm ²	0.09 g/4.5 cm ²
T_{FO} (min)	27	24	18	16
$T_{des.}$ (min)	3	6	12	14
SR_0 (g g ⁻¹)	0.85	0.85	0.85	0.85
ΔSR (g g ⁻¹)	0.099	0.380	1.371	2.249
m_{water} (mg)	99.0	228.0	274.2	202.4
$J_{app.}$ (LMH)	0.44	1.01	1.22	0.90

^a The hydrogel was in disc form contacting TFC membrane.

production rate of 1.04 LMH. The reduction of area density from 0.6 g/4.5 cm² to 0.2 g/4.5 cm² not only increased the desalinated water production rate, but reduced the amount of required hydrogel that can be a decline in hydrogel synthesis cost for possible future scale-up.

After the optimization of parameters including hydrogel composition, water diffusion conditions and area density, one FO–regeneration cycle duration is another important parameter for study to aim at the highest possible water production rate. As shown in Fig. 10, we reduced the duration of one FO–regeneration cycle from one hour to 30 minutes trying to make more use of the steep section in the swelling ratio–FO time curve to increase water flux. Similarly as seen from the key parameters summarized in Table 3, the area density of 0.2 g/4.5 cm² still generates the highest water production rate of 1.22 LMH. The distribution of 18 minutes in FO process and 12 minutes in regeneration process in a 30 minute cycle is also a macroscopic indication of a well balanced performance achieved by the PP444-6 SS hydrogel.

It is worth noting that the water production rate introduced in this work is different with the water flux values measured in FO process from other studies. Besides the advantages of no

draw agent back diffusion and no ensuing water polishing steps, another merit of thermally responsive hydrogels as draw agents is that theoretically only low grade thermal energy from waste heat or solar source is needed in desalination if electricity consumption for fluid motion is neglected. Although this water production rate of 1.22 LMH from polyionic liquid hydrogel is 5 times higher than that from PNIPAm-based hydrogel, admittedly, it is still comparatively lower than the water flux generated from other draw agent with smaller molecular weights. This is probably originated from severe dilutive concentration polarization, and improving the hydrogel–hydrogel and hydrogel–membrane contact conditions may further enhance the performance of hydrogels as draw agent. Interestingly, it was recently proven that shrinking hydrogel's dimension to less than 0.3 μm can produce a much higher water flux in FO process.³³ We believe that further optimizing the fabrication of thermally responsive polyionic liquid hydrogel would upgrade its performance, and hopefully make it more competent to other candidates as draw agent.

Conclusions

The thermally responsive polyionic liquid hydrogels have been synthesized and for the first time scrutinized as the draw agents in forward osmosis desalination. They can absorb water from feed solution faster than the PNIPAm-based hydrogels at room temperature, and squeeze absorbed water out at temperatures higher than the LCST. The thermally responsive ionic liquid can copolymerize with other species to subtly tune the balance of performances in FO and regeneration processes. In addition, other factors that can influence the FO performances including the contact conditions between hydrogel particles as well as FO membrane structure were also improved. Furthermore, we for the first time proposed a criterion to assess a hydrogel's comprehensive performance as draw agent in FO desalination, which is by comparing the desalinated water production rate in reversible FO–regeneration cycles. With this criterion, tuning other extrinsic parameters including hydrogel area density and one FO–regeneration duration were also found possible to improve water production rate. Compared with the PNIPAm-based hydrogels, we have finally increased the water production rate by a factor of 5 after tuning these parameters. We

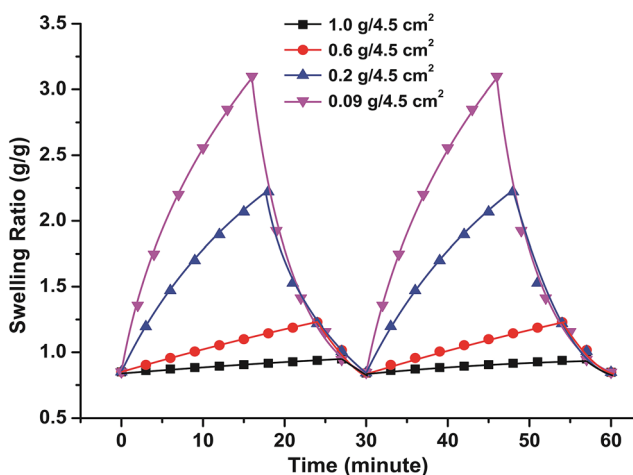


Fig. 10 The comprehensive performance of PP444-6 when one FO–regeneration cycle was fixed within 30 minutes. PP444-6 SS was used in disc form contacting TFC membrane.

believe and expect that by further optimization, especially the water permeation from membrane to hydrogel and within the hydrogel, it is not out of the question to further improve the water production rate to the extent that makes FO enabled by hydrogels more competitive in desalination.

Acknowledgements

The authors would like to thank the Environment and Water Industry Council (EWI) of Singapore for support *via* ECMG and SMTC of the Nanyang Environment and Water Research Institute (NEWRI) of Nanyang Technological University. Graduate scholarship awarded by Nanyang Technological University to the author of CYF is also gratefully acknowledged.

References

- 1 T. Cath, A. Childress and M. Elimelech, *J. Membr. Sci.*, 2006, **281**, 70–87.
- 2 B. Mi and M. Elimelech, *J. Membr. Sci.*, 2010, **348**, 337–345.
- 3 C. Klaysom, T. Y. Cath, T. Depuydt and I. F. Vankelecom, *Chem. Soc. Rev.*, 2013, **42**, 6959–6989.
- 4 L. Chekli, S. Phuntsho, H. K. Shon, S. Vigneswaran, J. Kandasamy and A. Chanan, *Desalin. Water Treat.*, 2012, **43**, 167–184.
- 5 Y. Cai, W. Shen, R. Wang, W. B. Krantz, A. G. Fane and X. Hu, *Chem. Commun.*, 2013, **49**, 8377–8379.
- 6 Q. Ge and T. S. Chung, *Chem. Commun.*, 2013, **49**, 8471–8473.
- 7 K. Lutchmiah, L. Lauber, K. Roest, D. J. H. Harmsen, J. W. Post, L. C. Rietveld, J. B. van Lier and E. R. Cornelissen, *J. Membr. Sci.*, 2014, **460**, 82–90.
- 8 D. Nakayama, Y. Mok, M. Noh, J. Park, S. Kang and Y. Lee, *Phys. Chem. Chem. Phys.*, 2014, **16**, 5319–5325.
- 9 R. Alnaizy, A. Aidan and M. Qasim, *J. Environ. Chem. Eng.*, 2013, **1**, 424–430.
- 10 M. L. Stone, C. Rae, F. F. Stewart and A. D. Wilson, *Desalination*, 2013, **312**, 124–129.
- 11 Z. Liu, H. Bai, J. Lee and D. D. Sun, *Energy Environ. Sci.*, 2011, **4**, 2582–2585.
- 12 Q. Zhao, N. Chen, D. Zhao and X. Lu, *ACS Appl. Mater. Interfaces*, 2013, **5**, 11453–11461.
- 13 C. X. Guo, D. Zhao, Q. Zhao, P. Wang and X. Lu, *Chem. Commun.*, 2014, **50**(55), 7318–7321.
- 14 J. Hopfner, C. Klein and M. Wilhelm, *Macromol. Rapid Commun.*, 2010, **31**, 1337–1342.
- 15 W. Ali, B. Gebert, T. Hennecke, K. Graf, M. Ulbricht and J. S. Gutmann, *ACS Appl. Mater. Interfaces*, 2015, **7**, 15696–15706.
- 16 S. Zhao, *Environ. Sci. Technol.*, 2014, **48**, 4212–4213.
- 17 H. Wang, J. Wei and G. P. Simon, *Environ. Sci. Technol.*, 2014, **48**, 4214–4215.
- 18 D. Li, X. Zhang, J. Yao, G. P. Simon and H. Wang, *Chem. Commun.*, 2011, **47**, 1710–1712.
- 19 S. Hirotsu, Y. Hirokawa and T. Tanaka, *J. Chem. Phys.*, 1987, **87**, 1392–1395.
- 20 D. Li, X. Zhang, J. Yao, Y. Zeng, G. P. Simon and H. Wang, *Soft Matter*, 2011, **7**, 10048–10056.
- 21 Y. Zeng, L. Qiu, K. Wang, J. Yao, D. Li, G. P. Simon, R. Wang and H. Wang, *RSC Adv.*, 2013, **3**, 887–894.
- 22 A. Razmjou, M. R. Barati, G. P. Simon, K. Suzuki and H. Wang, *Environ. Sci. Technol.*, 2013, **47**, 6297–6305.
- 23 H. Zhang, J. Li, H. Cui, H. Li and F. Yang, *Chem. Eng. J.*, 2015, **259**, 814–819.
- 24 A. Zhou, H. Luo, Q. Wang, L. Chen, T. C. Zhang and T. Tao, *RSC Adv.*, 2015, **5**, 15359–15365.
- 25 A. Razmjou, Q. Liu, G. P. Simon and H. Wang, *Environ. Sci. Technol.*, 2013, **47**, 13160–13166.
- 26 Y. Cai, W. Shen, S. L. Loo, W. B. Krantz, R. Wang, A. G. Fane and X. Hu, *Water Res.*, 2013, **47**, 3773–3781.
- 27 J. Wei, C. Qiu, C. Y. Tang, R. Wang and A. G. Fane, *J. Membr. Sci.*, 2011, **372**, 292–302.
- 28 A. Razmjou, G. P. Simon and H. Wang, *Chem. Eng. J.*, 2013, **215–216**, 913–920.
- 29 B. Ziolkowski and D. Diamond, *Chem. Commun.*, 2013, **49**, 10308–10310.
- 30 E. C. Cho, J. Lee and K. Cho, *Macromolecules*, 2003, **36**, 9929–9934.
- 31 W. Li and P. Wu, *Polym. Chem.*, 2014, **5**(19), 5578–5590.
- 32 A. Razmjou, Q. Liu, G. P. Simon and H. Wang, *Environ. Sci. Technol.*, 2013, **47**, 13160–13166.
- 33 Y. Hartanto, S. Yun, B. Jin and S. Dai, *Water Res.*, 2015, **70**, 385–393.